International Journal of Mass Spectrometry 343–344 (2013) 15–22

Contents lists available at SciVerse ScienceDirect

International Journal of Mass Spectrometry

journal homepage: www.elsevier.com/locate/ijms

Phospholipid analyses by MALDI-TOF/TOF mass spectrometry using 1,5-diaminonaphthalene as matrix

Wei Dong[1], Qing Shen[1], Joewel T. Baibado, Yimin Liang, Ping Wang, Yeqing Huang, Zhifeng Zhang, Yixuan Wang, Hon-Yeung Cheung*

Food & Drug Research Laboratory, Department of Biology and Chemistry, City University of Hong Kong, Hong Kong SAR, China

ARTICLE INFO

Article history:
Received 26 December 2012
Received in revised form 2 April 2013
Accepted 3 April 2013
Available online 11 April 2013

Keywords:
1,5-Diaminonaphthalene
<rk-italic>*Geobacillus stearothermophilus*</rk-italic>
MALDI-TOF/TOF
Phospholipids
Lipidomics

ABSTRACT

Phospholipids (PLs) are the major components of cellular membranes and play important biological roles. To effectively identify PL species and avoid chemical background interferences, 1,5-diaminonaphthalene (DAN) was introduced as a matrix in this study. A systematic evaluation of three established matrix substances, especially 2,5-dihydroxybenzoic acid (DHB) and 9-aminoacridine hemihydrate (9AA) as reference compounds, for phospholipid (PL) analysis was performed. Spectra of all analytes (phosphocholine (PC) in positive ion mode, the rest in negative ion mode) using DAN as the matrix showed only protonated/deprotonated analyte signals. Moreover, the spectra were totally devoid of any matrix related signals. In addition, ionization efficiency of PLs using DAN as matrix was evaluated, and improved signal intensities of analytes with low laser energy were produced, making DAN a versatile and sensitive reagent for PL analysis. DAN was also successfully applied to the PLs identification of *Geobacillus stearothermophilus*, in which phosphatidylethanolamine (PE) and phosphatidylglycerol (PG) were found to be the major classes. All the results indicate that DAN is a promising matrix for high-speed and effective lipidomics study by MALDI-TOF/TOF-MS.

1. Introduction

Among the various cellular metabolites, lipids are the leading molecules to be explored by omics-based studies, known as lipidomics [1]. Lipids and their metabolites play a vital role in a variety of biological processes including energy storage, cell signaling, antiviral protection, and as the structure to prevent alveolar collapse. Phospholipids (PLs), defined as glycerol-phosphate derivatives, are major components of cellular membranes (50–60% of lipid mass) and fulfill a variety of functions in cell signaling, cell growth and death. In bacteria and eukaryotic cells, PLs are constituted by straight-chain fatty acids linked to glycerol by ester bonds or/and ether bonds. Due to their structural diversity, it is therefore advantageous to acquire both positive and negative ion mode spectra from each analyzed sample provided that mass resolution, mass accuracy and the analysis throughput remain uncompromised [2].

Several protocols are available for lipid analysis, and common approaches are based on thin-layer chromatography (TLC) [3], high performance liquid chromatography (HPLC) [4], and shotgun method coupled to mass spectrometry (MS) [5]. Among the most advantageous "soft-ionization" techniques available today, electrospray ionization (ESI) MS has been widely employed for lipid analysis [6]. However, despite the more frequent use of this approach, MALDI-MS shows advantages over ESI-MS, characterized by excellent sensitivity, high tolerance against salts and sample impurities, and instrumental robustness, making it a promising alternative for high-through lipidomics analysis in complex biological samples [7–12]. Unfortunately, due to the interference of chemical background noise, which is a typical obstacle for sensitive MALDI-MS detection of compounds in the low-mass-region, comparatively little attention has been paid to the field of lipidomics [13,14].

Efforts have been made to solve the problem of low-mass-region interference. One active field is the development of matrix-free approaches involving laser desorption/ionization (LDI) of analytes from a specific surface. For example, Northen et al. [15] introduced nanostructure-initiator mass spectrometry (NIMS), a tool allowing direct characterization of peptide microarrays, direct mass analysis of single cell, tissue imaging, and direct characterization of blood and urine. Alternatively, several new matrices have been studied [16–19], e.g., 2,5-dihydroxybenzoic acid (DHB), 4-nitroaniline (PNA) and 2,4,6-trihydroxyacetophenone (THAP). But to date, only few matrix substances like DHB have been extensively used for

* Corresponding author at: Department of Biology and Chemistry, City University of Hong Kong, Tat Chee Avenue 83, Kowloon, Hong Kong SAR, China.
Tel.: +852 3442 7746; fax: +852 2788 7406.
E-mail address: bhhonyun@cityu.edu.hk (H.-Y. Cheung).
[1] Both authors contributed equally to this work.

1387-3806/$ – see front matter © 2013 Elsevier B.V. All rights reserved.
http://dx.doi.org/10.1016/j.ijms.2013.04.004

analysis of diverse lipid classes by MALDI-MS, and recently, 9-aminoacridine (9AA) was demonstrated to be an efficient matrix for analyzing low molecular weight acid, but limited to negative mode and in use may sometimes generate certain alkali metal adduct ions [20]. An ideal matrix should be totally devoid of matrix-related ion, this would make spectral interpretation straightforward.

1,5-diaminonapthalene (DAN) has been characterized as a basic matrix and used previously as a MALDI matrix for peptide in-source decay (ISD) process activation and reduction of peptide disulphide bonds facilitated sequencing. Moreover, it has successfully been applied for lipidomic analysis by imaging mass spectrometry [21,22]. In the present study, comparing DHB and 9AA, we describe an optimized method by introducing DAN as the matrix substance for highly sensitive detection of PLs by MALDI time of flight/time of flight (TOF/TOF) in both positive and negative ionization modes. To explain the beneficial effects of this compound, mass spectra acquired from different matrices were investigated and compared. Meanwhile, DAN was applied to the detection of small amounts of PL extracts from *Geobacillus stearothermophilus* for examining its robustness and sensitivity.

2. Materials and methods

2.1. Regents and chemicals

1,2-Dimyristoyl-*sn*-glycero-3-phosphocholine (DMPC), 1,2-dipalmitoyl-*sn*-glycero-3-phosphoethanolamine (DPPE), 1,2-dipalmitoyl-*sn*-glycero-3-phosphoinositol (DPPI), 1,2-dimyristoyl-*sn*-glycero-3-phospho-L-serine, sodium salt (DMPS), 1,2-dimyristoyl-*sn*-glycero-phosphate, sodium salt (DMPA), 1,2-dipentadecanoyl-*sn*-glycero-3-[phosphor-rac(1-glycerol)], and sodium salt (DPPG) were purchased from Avanti Polar Lipids (Alabama, USA). 2,5-dihydroxybenzoic acid (DHB), 9-aminoacridine hemihydrate (9AA), and 1,5-diaminonapthalene (DAN) were purchased from Sigma–Aldrich (St. Louis, MO, USA). HPLC grade chloroform, methanol, and acetonitrile were purchased from Fisher Scientific (Waltham, MA, USA). Water with a resistivity of 18 MΩ cm^1 was purified using a Milli-Q system from Millipore (Billerica, MA, USA). Purchased chemicals and solvents were obtained in the highest quality and used without additional purification.

2.2. Lipid extraction

G. stearothermophilus NCTC 10003 was cultured in the medium as described previously [23]. The strain was grown in a 5 L Winpact bench-top fermentor (Major Science, USA) at 60 °C, 300 rpm. Cell broth at middle exponential phase (optical density at 600 nm of ~0.6) was harvested by centrifugation at 6000 × *g* for 10 min, and the pellet was stored at −20 °C.

Lipids were extracted from *G. stearothermophilus* samples according to a modified version of the Bligh and Dyer method. Briefly, 0.1 g cell sample was accurately weighed in a 2 mL polytetrafluoroethylene tube, and mixed with 1.2 mL of $CHCl_3$/MeOH (2/1, v/v) solution. After extracting ultrasonically for 10 min, a portion of 0.4 mL water was added to separate the phase. Then, the mixture was centrifuged at 8000 × *g* for 10 min, and the lower organic phase was recovered and transferred to a new glass tube. The aqueous phase was re-extracted with 0.8 mL of $CHCl_3$ another two times and then handled as described before. The collected organic phases were combined and evaporated under nitrogen flow. Dried lipid extracts were dissolved in 1.0 mL of $CHCl_3$/MeOH (2:1, v/v) and stored in the dark at −80 °C. It is worth a mention that in order to minimize the risk of oxidation of the polyunsaturated fatty acids or lipid hydrolysis during the process of isolation, it is always recommended that the extraction process of lipids should be completed at low temperature (4 °C) as soon as possible after cell collection.

2.3. MALDI mass spectrometry

For MALDI-MS analysis, 5 mg/mL DAN was freshly prepared in isopropanol/acetonitrile (60/40, v/v) and mixed with an equal volume of sample solution before deposition onto the MALDI target. Much care should be taken when preparing DNA due to its potential carcinogenicity [24]. DHB and 9AA were also used as matrices. DHB was used as 30 mg/mL solution in methanol, whereas a 10 mg/mL solution of 9AA was prepared in isopropanol/acetonitrile (60/40, v/v), an optimized condition developed by Sun et al. [25]. Lipid extracts and phospholipid standard solutions were individually premixed 1:1 (v/v) with DHB, 9AA, and DAN, respectively, and subsequently applied onto a MALDI target plate.

All mass spectra shown were obtained using an Applied Biosystems 4800 MALDI-TOF/TOF mass spectrometer from (AB Sciex, Foster City, CA) equipped with a 200 Hz tripled-frequency Nd:YAG pulsed laser with 355 nm wavelength. Measurements were performed in MS or MS/MS mode by MALDI-TOF/TOF in either positive or negative ion reflection mode at an accelerating potential of 20 kV. A delayed ion extraction time of 450 ns was selected according to the mass range under observation (*m/z* 400–1200) allowing for baseline isotopic mass resolution. Mass spectra were obtained applying a laser energy adjusted up to 5–10% above threshold irradiation according to the manufacturer's nominal scale. An integrated video imaging system (~25× magnification) allowed direct observation of the sample spots under investigation. External mass calibration was achieved using mixture of phospholipid standard compounds described above. MS data acquisition was performed by 4000 Series Explorer, version 3.5.2 program.

2.4. Data analysis

MALDI-TOF MS data analysis was performed by the manufacturer supplied instrument software Data Explorer v.4.9 (Applied Biosystems) using the Savitzky–Golay smoothing algorithm. Lipid characterization was performed by comparing accurate mass measurements with the LIPID MAPS prediction tool (http://www.lipidmaps.org/tools/index.html). Values were displayed as mean ± standard deviation (SD) of at least triplicate measurements ($n \geq 3$).

3. Results and discussion

3.1. MALDI-TOF MS of DAN

The photochemical properties of DAN in tetrahydrofuran were previously studied by Wang [26]. The absorption maximum is centered at 330–350 nm in their spectra, which is assigned to the $n \rightarrow \pi^*$ electronic transition due to electron transfer from nitrogen lone pair to the π^* orbital of the naphthalene group. The UV–vis spectral absorption profile of DAN in solid state undergoes a red shift, which makes the DAN able to absorb the Nd:YAG laser wavelength (355 nm). Meanwhile, due to its strong UV absorption, rather low laser powers and much lower matrix concentrations are required. Fig. 1 showed the MALDI spectra of DAN in both positive and negative ion mode. DAN favored as the existence of a radical cation ($MH^{+\bullet}$ ion, *m/z* 157.8) in the gas phase, which was contrary to what is usually observed with other matrix (showing the favored formation of MH^+ ion). Further ions, presenting at *m/z* 299, 314, and 326, were considered to have originated from the radical induced reaction with neutral DAN molecules, but not simple DAN clusters

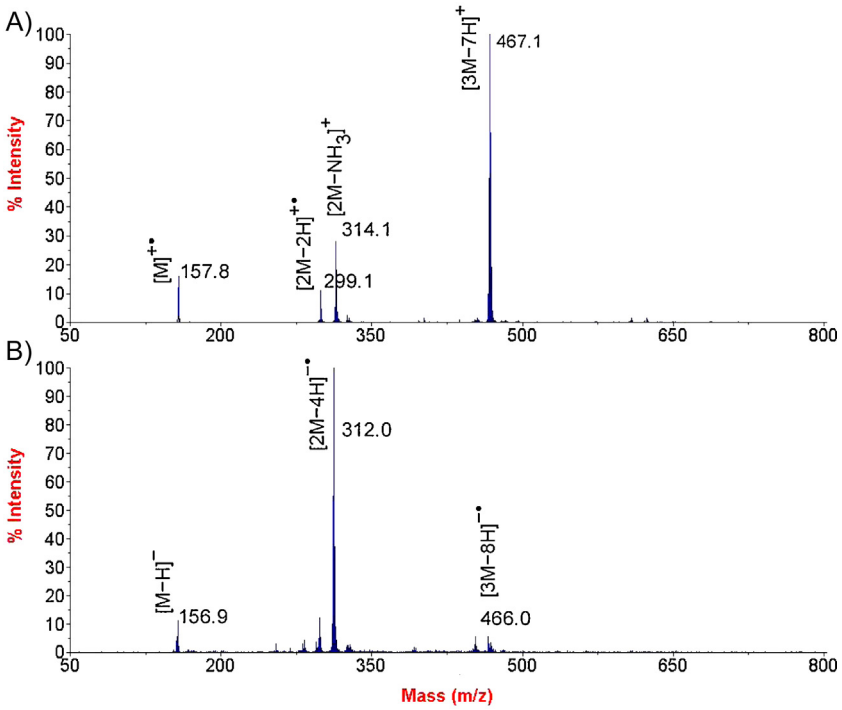

Fig. 1. Matrix assisted laser desorption ionization (MALDI) time of flight/time of flight mass spectrometry (TOF/TOF–MS) spectra of DAN in (A) positive ion mode and (B) negative ion mode.

[27]. This observation agrees as well with previous reports. In negative mode (Fig. 1B), the precursor ions of DAN were detected at *m/z* 155.9 and 156.9 at low mass range. We speculate thismass loss was derived from a reduction reaction involving the amino groups of DAN. Such a proton donating function of DAN was confirmed to be related to a reaction similar to that of a Bronsted-Lowry acid by Fukuyama [28]. The dominate ion in the full spectra was at *m/z* 312.0. Similar to that in positive ion mode, this ion was generated by a radical anion ($[M\text{-}2H]^{\bullet -}$) induced reaction with a neutral DAN molecule. In addition, ions originated from three DAN molecules were also observed at *m/z* 451 and 462. No other further appreciable decomposition and extensive cluster formation could be seen from the MALDI experiments. Therefore, DAN was shown to be suitable for analysis of phospholipids, whose mass charge ratios are usually more than 650.

3.2. Matrix comparison for PLs ionization behavior

PC and PE were selected as two representative PL classes and studied individually, because they accumulate in significant amounts in cells, tissues and body fluids. DHB and 9AA were chosen for performance comparison with that of DAN, since DHB is currently the most popular matrix used for MALDI mass analysis of lipids and other carbohydrates, while 9AA is a very promising negative ion matrix and has already been used for the detection of acidic lipids [20].

Figs. 2 and 3 showed selected positive and negative ion MALDI-TOF/TOF mass spectra of isolated DMPC and DPPE in order to illustrate the effect of DAN and the polarity mode. DMPC, with its quaternary amine, stabilized a positive charge quite strongly. Moreover, previous studies have shown that PC can inhibit the detection of other phospholipids in positive ion mode due to their easy ionization properties [29]. Its spectra in DAN (positive ion mode, Fig. 2B) provided exclusively intense $[M+H]^+$ and very minor $[M+Na]^+$. While in the spectra using DHB as matrix, the sodium adduct ion was significantly intensive [30], with intensity higher than 20% (Fig. 2C), which reduced sensitivity of detection due to signal splitting. When using 9AA as the matrix, the spectra were similar to those using DAN as the matrix, but it required much higher laser intensity(>6000). In the negative mode using DAN (Fig. 2D), the DMPC related ions occurred only after elimination of methyl group or other cations. For example, the most abundant ion at *m/z* 662 was $[M{-}CH_3]^-$, generated by charged quaternary amine induced in source fragmentation. The ions at *m/z* 591 and 617 were tentatively speculated to be $[M{-}CH_2{=}CHN^+(CH_3)_3{-}H]^-$ and $[M{-}HN^+(CH_3)_3{-}H]^-$, respectively. This speculation was further approved by MS^2 experiments, and the MS^2 spectra are shown in Fig. S1 (see Supporting Information). In the product ion spectra of the precursor at *m/z* 591, the most intense ion was at *m/z* 363, corresponding to the loss of an acyl chain (14:0) from its deprotonated molecule. The peak at *m/z* 227 was the ionized acyl chain (14:0) itself, while the peak at 79 was the diagnostic ion of $[PO_3]^-$. In the product ion spectra of the precursor at *m/z* 617 (Fig. S2, see Supporting Information), the ionized acyl chain (14:0) became the most abundant ion, while the intensity of its counterpart ($[617\text{–}227\text{–}H]^-$) was only about 10%. The peak at *m/z* 123 indicated the existence of the structure $[HOPO_3CH{=}CH_2]^-$ in its precursor ion. All of the fragment ions were consistent with the assignment of their precursors. The spectra of 9AA (Fig. 2E) was very similar to that of DAN, in which the ions described above were reduced, but some matrix adduct ions appeared, like the precursor ion at *m/z* 712. However, in the case of DHB (Fig. 2F), the spectra gave an exclusively intense DHB adduct peak ($[M+DHB{-}H]^-$) at *m/z* 830 [31]. A MS^2 experiment of DMPC was also conducted and no significant difference was observed in the spectra. Therefore, positive ion mode combined with the DAN matrix seems to be the optimum condition for DMPC detection.

In the case of DPPE (positive ion mode, Fig. 3), it behaved totally different to that of DMPC when DAN was used as the MALDI matrix, since no $[M+H]^+$ ion could be observed directly. Instead, the spectra were filled with alkali adduct ions, DAN adduct ions, and in source fragment ions, which markedly complicated spectral complexity

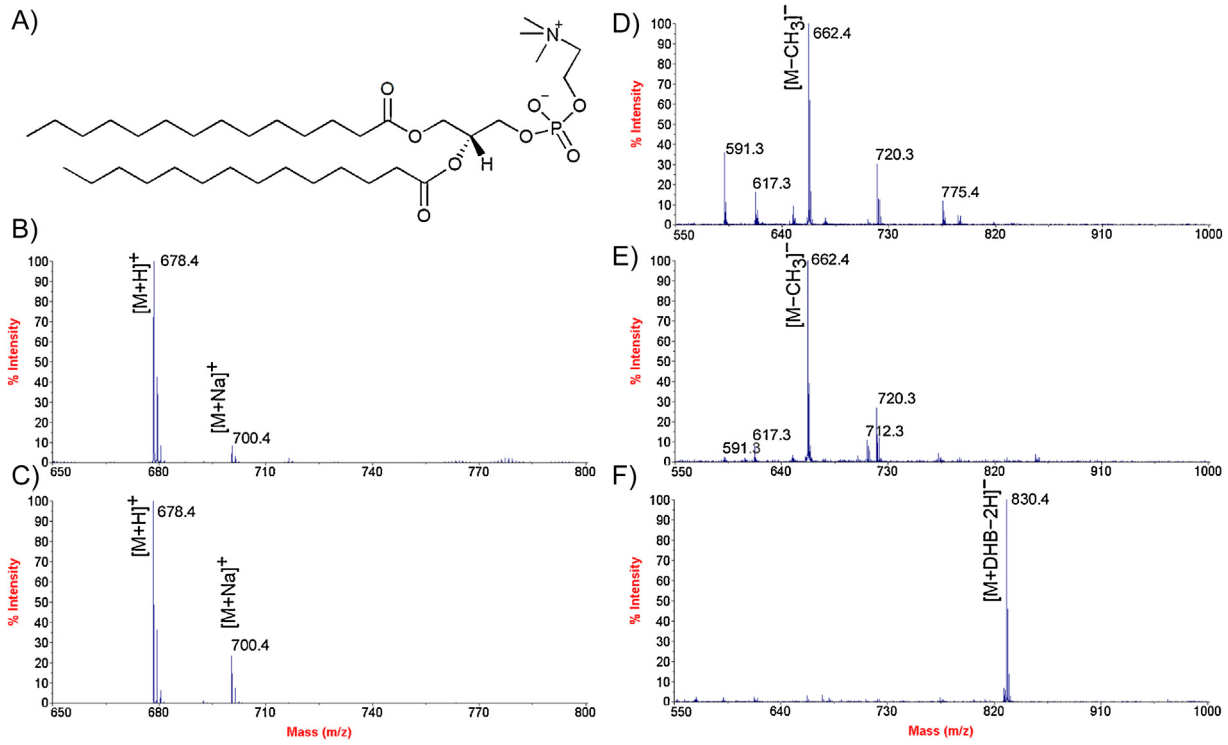

Fig. 2. (A) DMPC chemical structure, and MALDI TOF/TOF-MS spectra relevant to DMPC with (B) DAN in positive ion mode, (C) DHB in positive ion mode, (D) DAN in negative ion mode, (E) 9AA in negative ion mode, and (F) DHB in negative ion mode.

and data analysis. As shown in Fig. 3B, the peaks with *m/z* 686 and 708 were the two most abundant ions and assigned to be $[M+Na]^+$ and $[M+2Na-H]^+$, respectively, while, the peaks in the mass spectra with *m/z* 702 and 724 were corresponding to $[M+K]^+$ and $[M+Na+K-H]^+$, with comparatively lower intensity. The observed fragment ions at nominated *m/z* 619 and 647 were attributed to partial loss of the head group, identified as $[M-aziridine-H]^+$ and $[M-NH_3+H]^+$, respectively. Their detailed fragment pathways were

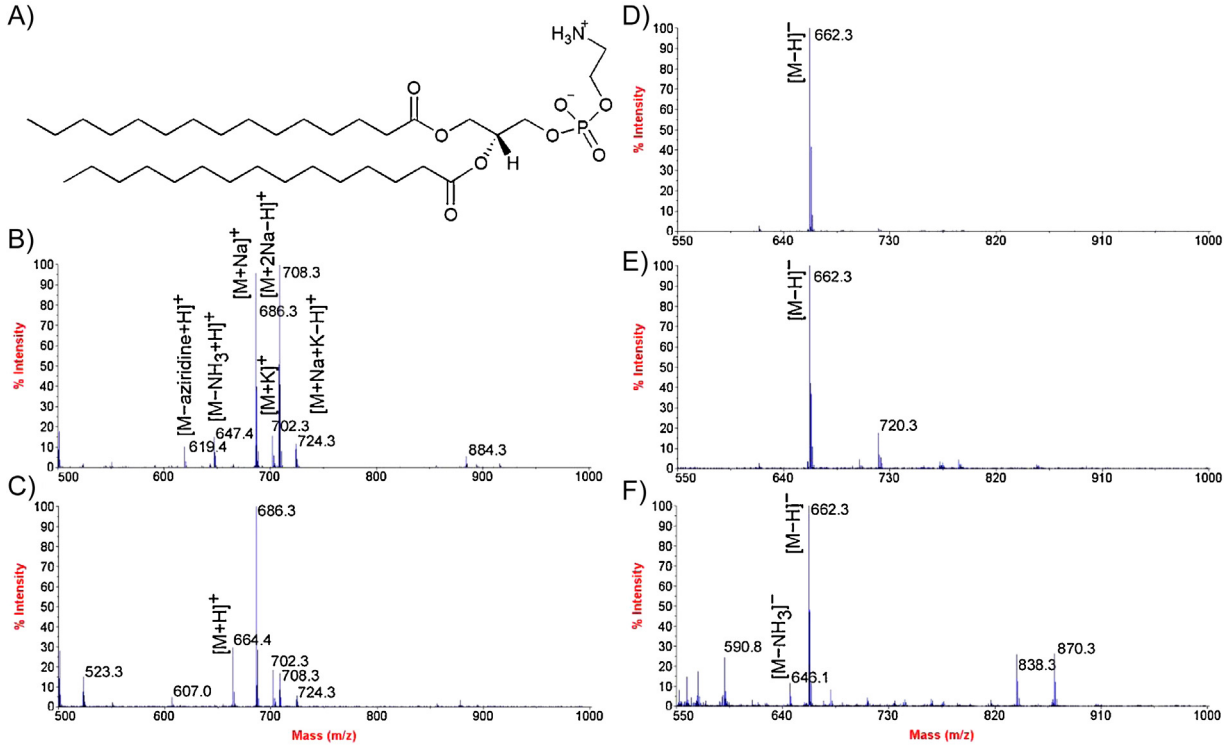

Fig. 3. (A) DPPE chemical structure, and MALDI TOF/TOF-MS spectra relevant to DPPE with (B) DAN in positive ion mode, (C) DHB in positive ion mode, (D) DAN in negative ion mode, (E) 9AA in negative ion mode, and (F) DHB in negative ion mode.

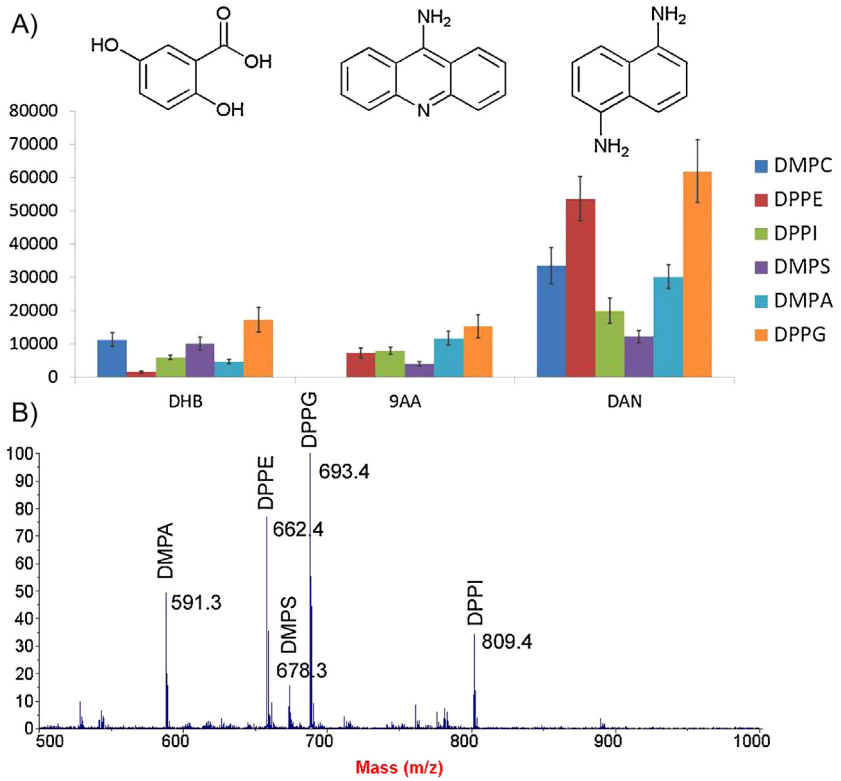

Fig. 4. Performance of (A) different MALDI matrixes for phospholipids detection and (B) representative spectrum relevant to a phospholipid mixture (DMPC, DPPE, DPPI, DMPS, DMPA, and DPPG). $[M\text{-}H]^+$ was analyzed for DMPC while $[M\text{-}H]^-$ for others. Values are mean SD of different sample analyses ($n = 4$).

previously proposed by Hsu and Turk [32]. In a similar manner to DAN matrix, the mass spectra of DPPE in DHB matrix exhibited alkali adduct ions (*m/z* 686, 702, 708, and 724), matrix adduct ions (*m/z* 878), and in source fragment ions (*m/z* 500, 523, and 607), although significant amounts of protonated DPPE ion $[M+H]^+$ at *m/z* 664 could be observed in the mass spectra (Fig. 3C). There was no signal observed in the spectra using 9AA as matrix in the positive ion mode. Therefore, the tested three MALDI matrices seem not suitable for analysis of PE in positive ion mode. In negative mode, PE species were ready to be ionized, since the phosphate hydroxyl group can be easily deprotonated (p*K*a = 5.70) while the amine group is only weakly acidic so it does not have any significant contribution in ionization. This was supported by a strong $[DPPE\text{—}H]^-$ion signal (*m/z* 662.5) (Fig. 3) and MS^2 spectra no matter using DAN, DHB or 9AA as MALDI matrix. It can be seen from Fig. 3D that the resulting spectra were much cleaner and that the DPPE ion peak (exclusively in the deprotonated form) was easily identified. Matrices adduct ions and in source fragment ions were prevalent in Fig. 3E and F, which would overlap with other PLs and complicate the data interpretation process. Thus, through the use of DAN, a single $[M\text{—}H]^-$ion was formed and desorbed with high efficiency in the absence of multiple adduct ions and matrix clusters in the negative ion mode. DPPI, DMPS, DMPA and DPPG were also studied individually and they could be well detected and identified in negative ionization mode.

3.3. Matrix comparison for PLs ionization efficiency

The efficiency of ionization of individual representative PL compounds was compared using three different types of matrices: DHB, 9AA and DAN. The PL mixture consisting of equal molar quantities of DMPC, DPPE, DPPI, DMPS, DMPA, and DPPG was selected to evaluate the signal-to-noise (S/N) ratio. It is known that ionization of PLs mainly depends on the polar head groups bearing different functional groups. Fig. 4A demonstrated the S/N ratios of each PL during our investigation. It is important to point out that the measurements of DMPC were obtained in positive ion mode, since PC is a more sensitively detectable PL species in protonated form as already stated. DHB showed many interfering peaks (although the S/N ratio of the target peak is high), while 9AA and DAN provided considerably better results under our experimental setup. However, the laser energy needed for DAN (~4000) was significantly less than that of 9AA (>6000). The S/N ratios of the rest of the five tested PLs were recorded in negative ion mode and a ca. 5–10 fold increase of mean signals could be observed by using DAN, in contrast to 9AA or DHB as MALDI matrix. The ionization efficiency of each matrix substance was totally different, for example, DHB provided comparatively lower DPPE and DMPA signals, while 9AA gave relative weak peak of DMPS. The S/N ratio of DPPG was the highest no matter which matrix was used. Fig. 4B demonstrated a representative spectrum of PL mixture in negative ion mode using DAN as matrix. The DPPE at *m/z* 662 and the DPPG at *m/z* 693 were the most abundant ions observed. The above results demonstrated that positive and negative ion MALDI spectra produced by matrix DAN had an improved signal intensity of analytes with low laser energy, making DAN a versatile and sensitive reagent for phospholipid analysis. This phenomenon may be attributed to that DAN is regarded as reductive chemical, whose hydrogen-donating ability is higher than DHB [33].

3.4. Application of DAN for PLs analysis in vitro

There has also been widespread interest in the development of methods for analyzing lipid profiles from bacteria for addressing questions of the important roles lipids played in the structures of cell membranes or in the various metabolic and communication processes within cells [34]. The thermophilic eubacterium *G. stearothermophilus* has been extensively used as a model to identify

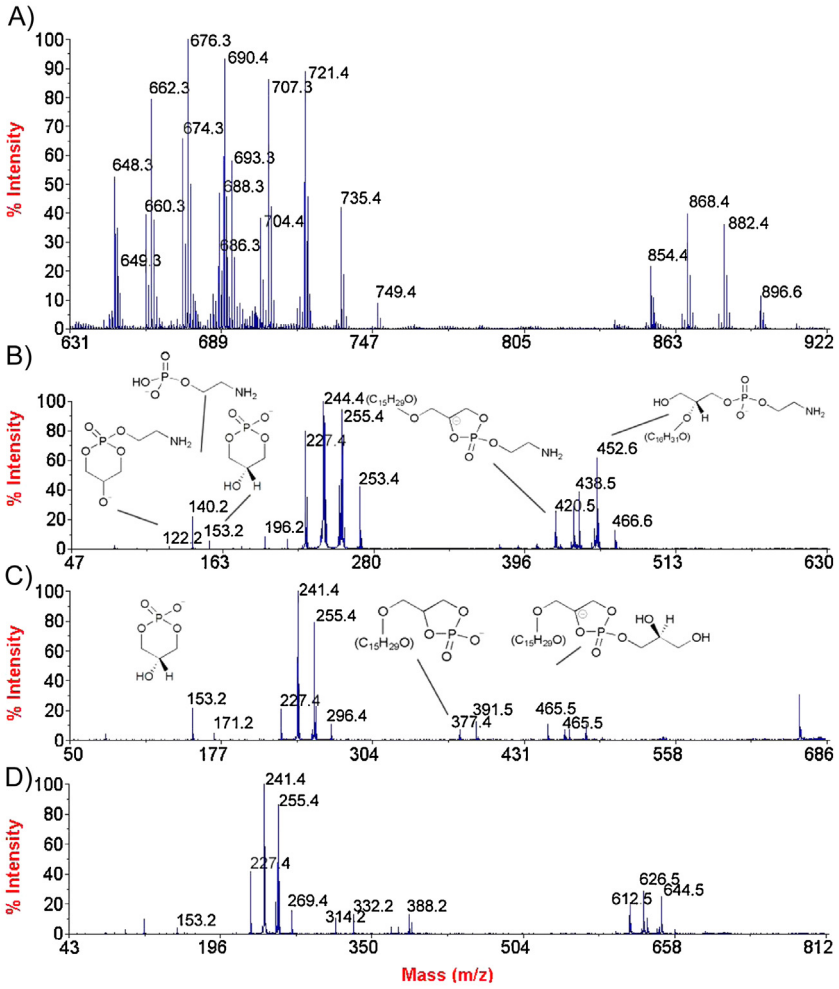

Fig. 5. (A) Negative ion MALDI TOF/TOF-MS spectra obtained using DAN as a matrix in the analysis of phospholipid extracts from culture of *G. stearothermophilus* strain NCTC 10003, and MS/MS spectra of precursor with *m/z* at (B) 676.3, (C) 707.3, and (D) 868.4.

membrane perturbing effects of lipophilic compounds, because its growth occurs at high temperatures, the risk of contamination is reduced, and results in bacterial cultures with high cell densities [34]. Therefore, PL extracts from the culture broth of *G. stearothermophilus* strain was studied to prove the potential of the proposed MALDI matrix in the analysis of real complex samples. The crude lipid extracts were directly spotted on the plate without any preseparation, and mass spectra were obtained by averaging 20 laser shots scanned across the sample spot. MALDI mass spectrometer was firstly operated in positive ion mode for monitoring the PC species. However, PC related ions were absent in the spectra, which theoretically lost a prominent fragment ion corresponding to neutral loss of 183 Da ($C_5H_{14}NPO_4$) along with the complementary protonated fragment ion at *m/z* 184. Instead, the spectra were filled with alkali adduct ions of PE and PG, which showed characteristic ions at *m/z* 164 and 195 in the MS^2 spectra, corresponding to the sodiated polar head-group $[Na^+(C_2H_5N)H_3PO_4]^+$ and $[Na^+(HOCH_2CHOHCH_2)H_3PO_4]^+$, respectively. These results are consistent with the previous findings that PE and PG are abundant in bacterial membranes while PC cannot be detected [34–35].

Improved results were obtained using negative ion mode as shown in Fig. 5A. The main ions were distributed within the range from *m/z* 645 to 920. The spectra obtained from DAN were similar to but much more than those from 9AA (Fig. S3, see Supporting Information). Most of the PL species were identified using MS^2 data, aided with the LIPID MAPS database (http://www.lipidmaps.org/) and MS prediction tool. In the spectra, significant even mass ions were observed and all of these ions were interpreted as PE species, which is in line with previous studies that PE is a major component in bacterial lipids [35]. For example, the predominant fragmentation of phospholipid with *m/z* 676 (Fig. 5B) contained a diagnostic peak at *m/z* 196, which corresponded to the loss of H_2O from glycerol phosphoethanolamine. The fragment ions at *m/z* 227, 241, 255, and 269 were speculated to be deprotonated acyl chain $C_{14:0}$, $C_{15:0}$, $C_{16:0}$, and $C_{17:0}$, respectively, indicating that at least two PE species with different acyl side chain compositions were overlapped at this precursor ion peak. The other fragment ions in the spectra also indicated the presence of PE, with *m/z* 466, 452 and 438 corresponding to the loss of acyl chain $C_{14:0}$, $C_{15:0}$ and $C_{16:0}$ as ketenes, respectively, and *m/z* 140 and 122, corresponding to the ethanolamine phosphate ion and ethanolamine phosphate ion with loss of H_2O, respectively. Therefore, PLs species at *m/z* 676 were speculated to be PE (14:0/17:0) and PE (15:0/16:0). As expected from the sample composition, *G. stearothermophilus* lipid extracts contained various PE species, including *m/z* 648, 660, 674, 686, 688, 690, and 704, which were identified based on MS^2 spectra and summarized in Tables 1 and S1 (see Supporting Information).

PG class is the second most abundant phospholipids in bacteria as reported [36]. Similar MS^2 spectra were observed for all of the significant odd mass ions observed. Fig. 5C showed representative MS^2 spectra of PG at *m/z* 707. The diagnostic fragmentation of phospholipids involved the cleavage of the phosphate–glycerol

Table 1
Attribution of the main ions observed in the spectra of Fig. 5A.

Class	Observed *m/z*	CN:DB[a]
PE	648.3	29:0
	660.3	28:1
	674.3	31:1
	676.3	31:0, 32:0[b]
	686.3	32:2
	688.3	32:1
	690.4	32:0, 33:0[b]
	704.4	33:0, 34:0[b]
PG	649.3	27:1
	707.3	31:0, 32:0[b]
	721.4	32:0, 33:0[b]
	735.4	33:0, 34:0[b]
	749.4	34:0, 35:0[b]
PE derivatives	854.4	30:0
	868.4	31:0
	882.4	32:0
	896.6	33:0

PE = phosphoethanolamine; PG = phosphatidylglycerol.
[a] CN:DB stands for the ratio between carbon number and double bonds.
[b] Plasmanyl/acyl PE (1-O-alkyl-2-acyl PE).

bond, resulting in the elimination of a characteristic phosphatidyl head-group, which was deprotonated and appeared at *m/z* 153. The spectra showed two predominant fragment ions at *m/z* 241 and 255, complying with the deprotonated acyl chain $C_{15:0}$ and $C_{16:0}$, respectively. The fragments at *m/z* 451 and 465 could be assigned to the loss of $C_{16:0}$ and $C_{15:0}$ fatty acids, while the fragment ions at *m/z* 377 and 391 were consistent with the further loss of the glycerol from *m/z* 451 and 465, respectively. Other precursors with *m/z* 649, 707, 721, 735, and 749 were identified as PG species and listed in Tables 1 and S1 (see Supporting Information).

In addition, there were even mass signals in the mass range from *m/z* 850 to 900, in which four significant precursors could be observed, including *m/z* 854, 868, 882, and 896. These ions were not matrix adducts since they appeared at the same mass-charge ratio even using DHB and 9AA as matrices. The MS^2 spectra, taking precursor ion at *m/z* 868 as an example (Fig. 5D), showed signals of acyl chain ions at *m/z* 227, 241, and 255, and the counterpart ions loss of one acyl chain as ketene from $[M-H]^-$, at *m/z* 626 and 644. Thus, this ion was speculated to be a PL derivative with linkage at the head group. The even *m/z* product ions at *m/z* 388, 332, and 314 aided our speculation, since these ions agreed with the mass weight of derived glycerol ethanolamine phosphate ion, derived ethanolamine phosphate ion, and derived ethanolamine phosphate ion with loss of H_2O. Notwithstanding that, assignment of all the peaks in the spectra was not the focus of this paper. We tentatively considered these ions as PE derivatives. A summary of the PL ions identified in the mass spectra for *G. stearothermophilus* using the MALDI-TOF/TOF data is given in Table 1.

Collectively, compared with DHB and 9AA as matrices, the intensity of the spectra from DAN was much higher, allowing the detection of individual PLs. Moreover, using DAN as the matrix produced definitely deprotonated ions without any matrix adducts which could contaminate the spectra from real samples and make difficulties to analyze PL species.

4. Conclusions

The discovery of novel matrix substances and constant improvements in sensitivity and reproducibility for phospholipidomics study using the MALDI-MS method for ionization is an active and dynamic area of research. Here, we present DAN as MALDI matrix for studying phospholipids including PC, PE, PI, PS, PA, and PG. Compared with conventional matrices such as DHB and 9AA, the results can be obtained using DAN even at much lower concentration. Absence of matrix related ions makes DAN ideal for studying phospholipids in the low mass weight region. The detailed evaluation of critical parameters including different matrix substances, PLs fragmentation behavior in gas phase, and the PLs ionization efficiency reveals crucial to acquire sufficiently high sensitivity and versatility for detection of different PL classes in positive and negative ionization modes. Finally, the combination of these essential factors was successfully applied to identify PLs from *G. stearothermophilus*. Considering the robustness and high throughput capability of MALDI-MS/MS, DAN with its remarkable properties has a great potential for lipidomics study of low concentration PLs.

Acknowledgments

The authors would like to thank the Hong Kong Chinese Materia Medica Standards (HKCMMS) fund (CityU Project No. 9211024) from the Department of Health, Hong Kong SAR Government. Q.S., W.D., and Y.L. also thank the Hong Kong RGC for supporting their studentships.

Appendix A. Supplementary data

Supplementary data associated with this article can be found, in the online version, at http://dx.doi.org/10.1016/j.ijms.2013.04.004.

References

[1] E.A. Dennis, Lipidomics joins the omics evolution, Proceedings of the National Academy of Sciences of the United States of America 7 (2009) 2089–2090.
[2] K. Schuhmann, R. Almeida, M. Baumert, R. Herzog, S.R. Bornstein, A. Shevchenko, Shotgun lipidomics on a LTQ orbitrap mass spectrometer by successive switching between acquisition polarity modes, Journal of Mass Spectrometry 47 (2012) 96–104.
[3] G. Paglia, D.R. Ifa, C. Wu, G. Corso, R.G. Cooks, Desorption electrospray ionization mass spectrometry analysis of lipids after two-dimensional high-performance thin-layer chromatography partial separation, Analytical Chemistry 82 (2010) 1744–1750.
[4] U. Sommer, H. Herscovitz, F.K. Welty, C.E. Costello, LC-MS-based method for the qualitative and quantitative analysis of complex lipid mixtures, Journal of Lipid Research 47 (2006) 804–814.
[5] X. Han, K. Yang, R.W. Gross, Multi-dimensional mass spectrometry-based shotgun lipidomics and novel strategies for lipidomic analyses, Mass Spectrometry Reviews 31 (2012) 134–178.
[6] F.F. Hsu, J. Turk, R.M. Owens, E.R. Rhoades, D.G. Russell, Structural characterization of phosphatidyl-*myo*-inositol mannosides from *Mycobacterium bovis* bacillus calmette gúerin by multiple-stage quadrupole ion-trap mass spectrometry with electrospray ionization. II. Monoacyl- and diacyl-PIMs, Journal of the American Society for Mass Spectrometry 18 (2007) 479–492.
[7] S. Chen, N.A. Belikova, P.V. Subbaiah, Structural elucidation of molecular species of pacific oyster ether amino phospholipids by normal-phase liquid chromatography/negative-ion electrospray ionization and quadrupole/multiple-stage linear ion-trap mass spectrometry, Analytica Chimica Acta 735 (2012) 76–89.
[8] S. Chen, K.W. Li, Mass spectrometric identification of molecular species of phosphatidylcholine and lysophosphatidylcholine extracted from shark liver, Journal of Agricultural and Food Chemistry 55 (2007) 9670–9677.
[9] M. Pulfer, R.C. Murphy, Electrospray mass spectrometry of phospholipids, Mass Spectrometry Reviews 22 (2003) 332–364.
[10] R.C. Murphy, P.H. Axelsen, Mass spectrometric analysis of long-chain lipids, Mass Spectrometry Reviews 30 (2011) 579–599.
[11] Q. Shen, Y. Wang, L. Gong, R. Guo, W. Dong, H.Y. Cheung, Shotgun lipidomics strategy for fast analysis of phospholipids in fisheries waste and its potential in species differentiation, Journal of Agricultural and Food Chemistry 60 (2012) 9384–9393.
[12] B. Fuchs, R. Süß, J. Schiller, An update of MALDI-TOF mass spectrometry in lipid research, Progress in Lipid Research 49 (2010) 450–475.
[13] H.J. Wang, S.N. Jackson, A.S. Woods, Direct MALDI-MS analysis of cardiolipin from rat organs sections, Journal of the American Society for Mass Spectrometry 18 (2007) 567–577.
[14] K.M. McAvey, B. Guan, C.A. Fortier, M.A. Tarr, R.B. Cole, Laser-induced oxidation of cholesterol observed during MALDI-TOF mass spectrometry, Journal of the American Society for Mass Spectrometry 22 (2011) 659–669.
[15] T.R. Northen, O. Yanes, M.T. Northen, D. Marrinucci, W. Uritboonthai, J. Apon, S.L. Golledge, A. Nordstrom, G. Siuzdak, Clathrate nanostructures for mass spectrometry, Nature 449 (2007) 1033–1036.

[16] C.D. Calvano, S. Carulli, F. Palmisano, 1H-Pteridine-2, 4-dione (lumazine): a new MALDI matrix for complex (phospho) lipid mixtures analysis, Analytical and Bioanalytical Chemistry 398 (2010) 499–507.
[17] C.L. Carter, C.W. McLeod, J. Bunch, Imaging of phospholipids in formalin fixed rat brain sections by matrix assisted laser desorption/ionization mass spectrometry, Journal of the American Society for Mass Spectrometry 22 (2011) 1991–1998.
[18] H. Yang, J. Wang, F. Song, Y. Zhou, S. Liu, Isoliquiritigenin (4, 2′, 4′-trihydroxychalcone): a new MALDI matrix with outstanding properties for the analysis of neutral oligosaccharides, Analytica Chimica Acta 701 (2011) 45–51.
[19] G. Stubiger, O. Belgacem, P. Rehulka, W. Bicker, B.R. Binder, V. Bochkov, Analysis of oxidized phospholipids by MALDI mass spectrometry using 6-aza-2-thiothymine together with matrix additives and disposable target surfaces, Analytical Chemistry 82 (2010) 5502–5510.
[20] M. Eibisch, J. Schiller, Sphingomyelin is more sensitively detectable as a negative ion than phosphatidylcholine: a matrix-assisted laser desorption/ionization time-of-flight mass spectrometric study using 9-aminoacridine (9-AA) as matrix, Rapid Communications in Mass Spectrometry 25 (2011) 1100–1106.
[21] K.A. Berry, J.A. Hankin, R.M. Barkley, J.M. Spraggins, R.M. Caprioli, R.C. Murphy, MALDI imaging of lipid biochemistry in tissues by mass spectrometry, Chemical Reviews 111 (2011) 6491–6512.
[22] A. Thomas, J.L. Charbonneau, E. Fournaise, P. Chaurand, Sublimation of new matrix candidates for high spatial resolution imaging mass spectrometry of lipids: enhanced information in both positive and negative polarities after 1,5-diaminonapthalene deposition, Analytical Chemistry 84 (2012) 2048–2054.
[23] H.Y. Cheung, L. Vitkovic, M.R.W. Brown, Dependence of *Bacillus stearothermophilus* spore germination on nutrient depletion and manganese, Microbiology 128 (1982) 2403–2409.
[24] E. Bingham, B. Cohrssen, C.H. Powell, Patty's Toxicology, vols. 1–9, 5th ed., John Wiley & Sons, New York, NY, 2001V4 1064.
[25] G. Sun, K. Yang, Z. Zhao, S. Guan, X. Han, R.W. Gross, Matrix-assisted laser desorption/ionization time-of-flight mass spectrometric analysis of cellular glycerophospholipids enabled by multiplexed solvent dependent analyte-matrix interactions, Analytical Chemistry 80 (2008) 7576–7585.
[26] G. Wang, Optical and electrochemical investigation of diaminonaphthalene derivatives, Synthetic Metals 160 (2010) 599–603.
[27] L. Molin, R. Seraglia, F.R. Dani, G. Moneti, P. Traldi, The double nature of 1,5-diaminonaphthalene as matrix-assisted laser desorption/ionization matrix: some experimental evidence of the protonation and reduction mechanisms, Rapid Communications in Mass Spectrometry 25 (2011) 3091–3096.
[28] Y. Fukuyama, S. Iwamoto, K. Tanaka, Rapid sequencing and disulfide mapping of peptides containing disulfide bonds by using 1,5-diaminonaphthalene as a reductive matrix, Journal of Mass Spectrometry 41 (2006) 191–201.
[29] S.N. Jackson, H.Y. Wang, A.S. Woods, Direct profiling of lipid distribution in brain tissue using MALDI-TOF MS, Analytical Chemistry 77 (2005) 4523–4527.
[30] X. Shu, Y. Li, M. Liang, B. Yang, C. Liu, Y. Wang, J. Shu, Rapid lipid profiling of bacteria by online MALDI-TOF mass spectrometry, International Journal of Mass Spectrometry 71 (2012) 321–322.
[31] J. Schiller, R. Süss, M. Petković, O. Zschörnig, K. Arnold, Negative-ion matrix-assisted laser desorption and ionization time-of-flight mass spectra of complex phospholipid mixtures in the presence of phosphatidylcholine: a cautionary note on peak assignment, Analytical Biochemistry 309 (2002) 311–314.
[32] F.F. Hsu, J. Turk, Electrospray ionization with low-energy collisionally activated dissociation tandem mass spectrometry of glycerophospholipids: mechanisms of fragmentation and structural characterization, Journal of Chromatography B 877 (2009) 2673–2695.
[33] M. Sakakura, M. Takayama, In-source decay and fragmentation characteristics of peptides using 5-aminosalicylic acid as a matrix in matrix-assisted laser desorption/ionization mass spectrometry, Journal of the American Society for Mass Spectrometry 21 (2010) 979–988.
[34] J. Giddena, J. Denson, R. Liyanage, D.M. Ivey, J.O. Lay Jr., Lipid compositions in *Escherichia coli* and *Bacillus subtilis* during growth as determined by MALDI-TOF and TOF/TOF mass spectrometry, International Journal of Mass Spectrometry 283 (2009) 178–184.
[35] G.L. Card, Metabolism of phosphatidylglycerol, phosphatidylethanolamine, and cardiolipin of *Bacillus stearothermophilus*, Journal of Bacteriology 114 (1973) 1125–1137.
[36] W. Dowhan, Molecular basis for membrane phospholipid diversity: why are there so many lipids, Annual Review of Biochemistry 66 (1997) 199–232.